

Knot Topology of Exceptional Point and Non-Hermitian No-Go Theorem

Haiping Hu,^{1,*} Shikang Sun,^{1,2} and Shu Chen^{1,2,3}

¹*Beijing National Laboratory for Condensed Matter Physics,*

Institute of Physics, Chinese Academy of Sciences, Beijing 100190, China

²*School of Physical Sciences, University of Chinese Academy of Sciences, Beijing 100049, China*

³*Yangtze River Delta Physics Research Center, Liyang, Jiangsu 213300, China*

Exceptional points (EPs) are peculiar band singularities and play a vital role in a rich array of unusual optical phenomena and non-Hermitian band theory. In this paper, we provide a topological classification of isolated EPs based on homotopy theory. In particular, the classification indicates that an n -th order EP in two dimensions is fully characterized by the braid group B_n , with its eigenenergies tied up into a geometric knot along a closed path enclosing the EP. The quantized discriminant invariant of the EP is the *writhe* of the knot. The knot *crossing number* gives the number of bulk Fermi arcs emanating from each EP. Furthermore, we put forward a non-Hermitian *no-go* theorem, which governs the possible configurations of EPs and their splitting rules on a two-dimensional lattice and goes beyond the previous fermion doubling theorem. We present a simple algorithm generating the non-Hermitian Hamiltonian with a prescribed knot. Our framework constitutes a systematic topological classification of the EPs and paves the way towards exploring the intriguing phenomena related to the enigmatic non-Hermitian band degeneracy.

Non-Hermitian (NH) systems are ubiquitous in physics [1–9], as epitomized by various photonic platforms with gain and loss [10–28]. One of the most remarkable features of NH systems is that they exhibit level degeneracy of their complex eigenenergies, called exceptional points (EPs) [29, 30]. At an EP, two or more eigenvalues, and their corresponding eigenvectors, simultaneously coalesce (i.e., the Hamiltonian is defective), giving rise to phenomena without any analogs in the Hermitian realm. The intriguing properties of EPs have been widely exploited such as in unconventional transmission or reflection [31], enhancing sensing [32–34], single-mode lasing [35, 36] and non-reciprocal phase transitions [37].

EPs can be categorized into different types [38]. An EP is of n -th order or n -fold (EP _{n}) if n eigenstates simultaneously coalesce, i.e., the Hamiltonian is diagonalized into an $n \times n$ Jordan normal form. Similar to the well-known Dirac point or Weyl point in Hermitian systems, EP can be characterized by assigning an integer invariant like the vorticity of eigenvalues [39] or discriminant number [40]. Such characterizations, however, are far from satisfactory and incomplete. First, EPs of different types (especially of higher-order) that cannot smoothly evolve from one to another may have the same integer invariant introduced before. Second, NH Hamiltonians generally have complex eigenenergies compared to Hermitian systems, bringing critical differences in their topological characterizations [41–45]. Near an EP, the energy levels may braid and tangle together; hence they cannot be captured solely by simple integer invariants. Moreover, the band braiding near an EP may induce novel types of EPs previously unidentified. Systematic classification and identification of EPs are still lacking.

In this paper, we formulate a homotopic classification of EPs in arbitrary dimensional NH systems (or generic parameter space), which enables the calculation of topo-

logical invariants using the machinery well-developed in algebraic topology. Particularly, in 2D, our main findings are: *i*) An isolated n -th order EP is fully characterized by braid group B_n , which reduces to integer group \mathbb{Z} for EP₂. The energy levels are tied up into a geometric knot along a closed encircling path [see Fig. 1]. The quantized vorticity (or discriminant number) and the number of bulk Fermi arcs emanating from the EP is the *writhe* and *crossing number* of the knot, respectively. *ii*) Furthermore, based on the classification, we put forward a NH no-go theorem that goes beyond the previous fermion doubling theorem based on the discriminant number. It dictates the possible configurations of EPs and their splitting rules on a 2D lattice. *iii*) To facilitate experimental realizations, we show how to generate a NH Hamiltonian hosting an EP of a prescribed knot pattern. Our framework bridges the NH physics, algebraic topology, and knot theory, and opens a broad avenue for investigating the exotic features of NH band degeneracies.

Homotopy classification.—Let us consider an n -band NH Hamiltonian $H(\mathbf{k}) = H(k_1, k_2, \dots, k_d)$ of d D system (or parameter space) and suppose an isolated n -fold EP located at $\mathbf{k} = 0$. At the EP, the Hamiltonian can be brought to the Jordan normal form (For simplicity, the EP is set at zero energy unless otherwise noted). Deviating from the EP, the energy levels are separated from each other. We denote the eigenvalues and corresponding eigenvectors of $H(\mathbf{k})$ as $X_n = (z_1, z_2, \dots, z_n; \psi_1, \psi_2, \dots, \psi_n)$. We note that an isolated EP in d D can be enclosed by a $(d-1)$ D sphere S^{d-1} . From the homotopy point of view, classifying the band structures near the EP is to find all the nonequivalent classes of the *non-based* maps from S^{d-1} to X_n , denoted as $[S^{d-1}, X_n]$.

The eigenvalue part is the configuration space of ordered n -tuples $\text{Conf}_n(\mathbb{C})$. As each eigenvector is unique

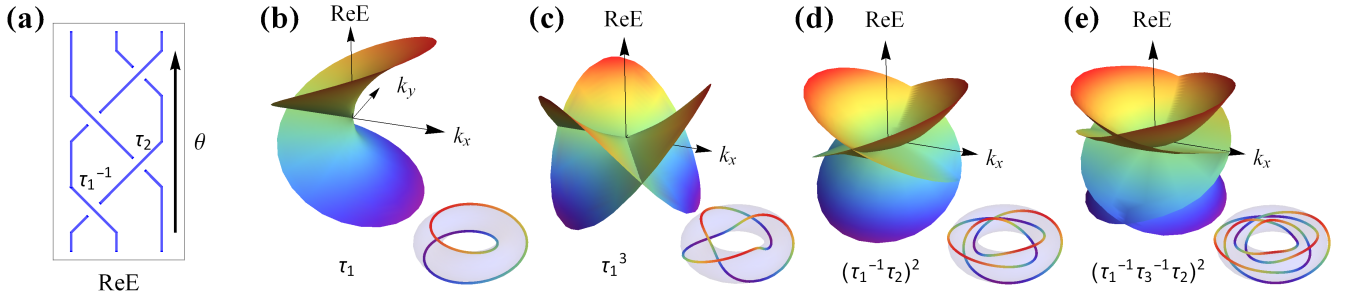


FIG. 1. Exceptional points (EPs) with energy-level braiding and knot topology. (a) Braid diagram marked by Artin's braid word notation: τ_i (τ_i^{-1}) represents the i -th strand crosses over/under the $i + 1$ -th strand when traveling upwards. Closure of the braid by identifying the up and bottom ends forms a knot (in this case, it is the figure-8 knot). (b)-(e) Band structures (real part) and their associated knots along a closed path enclosing the EP (lower panels) for some representative EPs. (b) EP₂ of unknot, braid word: τ_1 , the characteristic polynomial (ChP) is $\lambda^2 - z$; (c) EP₂ of trefoil knot, braid word: τ_1^3 , the ChP is $\lambda^2 - z^3$; (d) EP₃ of figure-8 knot, braid word $(\tau_1^{-1}\tau_2)^2$; (e) EP₄ of L6a1 link, braid word: $(\tau_1^{-1}\tau_3^{-1}\tau_2)^2$. The ChP for figure-8 knot is given by f_8 in the main text.

up to multiplying a nonzero phase factor, the eigenvector space (denoted as Ψ) is $\Psi \cong \mathrm{U}(n)/\mathrm{U}^n(1)$. By further removing the redundancy of permutation of eigenvalues (together with their associated eigenvectors), we have the classifying space $X_n \cong (\mathrm{Conf}_n \times \Psi)/S_n$, with S_n the symmetric group of degree n . Using the relations $\pi_1(\mathrm{Conf}_n) = \mathrm{PB}_n$ (pure braiding group) [46, 47] and $\pi_m(\mathrm{Conf}_n) = 0$ ($m \geq 2$) [48], and long sequence of homotopy relations [41, 42, 49], we have:

$$\pi_1(X_n) = \mathrm{B}_n, \quad d = 2; \quad (1)$$

$$\pi_2(X_n) = \mathbb{Z}^{n-1}, \quad d = 3; \quad (2)$$

$$\pi_{d-1}(X_n) = \pi_{d-1}(\mathrm{U}(n)), \quad d \geq 4. \quad (3)$$

For $d = 2, n = 2$, the homotopy group $\mathrm{B}_2 \cong \mathbb{Z}$, consistent with the previous characterization of EP₂ through vorticity [39] or discriminant number [40]. The above homotopy groups are all Abelian except for $d = 2, n \geq 3$, which is the braid group B_n . If we travel along a circle around a 2D EP, the energy levels braid together. Eq. (1) indicates that the topology of a 2D EP_n is entirely captured by such braiding pattern. Eq. (2) means a 3D EP_n is characterized by assigning a Chern number to each of the separable n bands, with the constraints that they sum to zero.

The non-based map relates to the homotopy group through the action of the fundamental group [49]:

$$[S^{d-1}, X_n] \cong \pi_{d-1}(X_n)/\pi_1(X_n). \quad (4)$$

The right-hand side is the orbit set. $[S^{d-1}, X_n]$ is not necessarily a group and usually decomposed into several distinct sectors, induced by the fundamental group. While the non-based homotopy can be worked out in a case-by-case manner, in 2D, $[S^1, X_n]$ is the conjugacy class of the braid group B_n [41–43]. In fact, choosing a different starting point on the encircling path may end up with another braid, which however, conjugate to the original one, hence they are in the same conjugacy class. In 3D,

$[S^2, X_n]$ is a collection of n integer Chern numbers. Due to the un-sortability of the complex energy levels, the two integer sets $[s_1, s_2, \dots, s_n]$ and $[s_{b_1}, s_{b_2}, \dots, s_{b_n}]$ (the set induced by the band permutation of any $b \in \pi_1(X_n)$) are identified as the same [41, 42].

Knot around EP.—In the following, we focus on 2D EPs. It turns out there is a one-to-one correspondence between the conjugacy class of braid group B_n and geometric knot in the solid torus [50], culminating in a *knot* classification of the EPs. Different types of EPs are represented by topologically distinct knots, thus characterized by knot invariants [43, 47], e.g., Jones polynomials [51]. Intuitively, let us take a closed path $\Gamma(\theta)$ ($\theta \in [0, 2\pi]$) surrounding the EP. Along Γ , the θ -dependent energy levels (z_1, z_2, \dots, z_n) trace n strands which tangle together in the 3D space spanned by $(\mathrm{ReE}, \mathrm{ImE}, \theta)$, as depicted in Fig. 1(a). The trajectory returns to itself to form a closed knot during the θ -evolution from 0 to 2π ($\theta = 0$ and $\theta = 2\pi$ is identical). The knot topology of a given EP is best represented using braid word. It can be determined by projecting the above energy-level strings onto the $\mathrm{ImE} = 0$ plane. As θ evolves, the strings undergo a sequence of crossings. In Artin's notation, we label a crossing as τ_i (τ_i^{-1}) if the i -th string crosses over (under) the $(i+1)$ -th string from left. τ_i satisfy the braid relation: $\tau_i \tau_j = \tau_j \tau_i$ for $|j - i| \geq 2$, and $\tau_i \tau_{i+1} \tau_i = \tau_{i+1} \tau_i \tau_{i+1}$. The entire level set is specified by a product of braid operators. For example, τ_1^n corresponds to twisting two level strands n times; $n = 1, 2, 3$ represents unknot, Hopf link, and Trefoil knot, respectively.

The knot near an EP can be regarded as the roots (or nodal set) of the characteristic polynomial (ChP). Denote $z = k_1 + ik_2$ and $H(z) = H(k_1, k_2)$, the ChP reads

$$f(\lambda, z) = \det[\lambda - H(z)] = \prod_{j=1}^n (\lambda - z_j). \quad (5)$$

The well-known complex polynomial for the (p, q) -torus knot is $f(\lambda, z) = \lambda^p - z^q$, with p roots $z_j = z^{q/p} e^{i2\pi(j-1)/p}$, ($j = 1, 2, \dots, p$). By tracing a closed path

around the EP, the energy levels wind q times around a circle in the interior of the torus, and p times around its axis of rotational symmetry. The simplest Hamiltonian realizing the (p,q) -torus knot can thus be chosen as:

$$H_{T_{p,q}} = \begin{pmatrix} 0 & 0 & 0 & (k_1 + ik_2)^q \\ 1 & 0 & 0 & 0 \\ 0 & \ddots & \ddots & 0 \\ 0 & 0 & 1 & 0 \end{pmatrix}_{p \times p}. \quad (6)$$

Figs. 1(b)(c) plot the band structures of EP_2 associated with $T_{2,1}$ (unknot) and $T_{2,3}$ (trefoil knot), respectively. The unknot case is the most studied EP_2 in the literature.

To find the Hamiltonian for an EP_n with a prescribed knot (denoted as \mathcal{K}), we need to construct the proper ChP $f(\lambda, z)$. As $\lambda, z \in \mathbb{C}$, $f(\lambda, z)$ defines a mapping from \mathbb{C}^2 to \mathbb{C} . The energy levels (z_1, z_2, \dots, z_n) are the nodal sets of the ChP and the EP_n is the isolated singularity located at $(\lambda, z) = (0, 0)$. Mathematically, the closure of the band braiding near the EP_n is the algebraic knot around the singular point. Akbulut and King [52] showed (albeit in a nonconstructive way) that any knot can arise as the knot around such a singular point of a polynomial in the context of complex hypersurfaces. From physical considerations, the ChP is semiholomorphic, i.e., it can be written as a complex polynomial in λ, z , and \bar{z} .

To this end, we need an ad hoc auxiliary polynomial $f_\theta : \mathbb{C} \times S^1 \rightarrow \mathbb{C}$, with the knot \mathcal{K} as its nodal set. As detailed in [43, 53], f_θ can be constructed intuitively from the Fourier parameterization of the braid diagram associated with the knot. Having obtained f_θ , we can replace $e^{\pm i\theta}$ with z and \bar{z} , respectively: $f(\lambda, z) = f_\theta(e^{i\theta} \rightarrow z; e^{-i\theta} \rightarrow \bar{z})$. In some cases, however, such an analytical continuum does not necessarily guarantee the EP_n is the isolated singular point of $f(\lambda, z)$. To overcome this issue, we slightly modify the ChP to take the following form ($g > 0$ is some integer) [54]:

$$f(\lambda, z) = (z\bar{z})^{ng} f\left(\frac{\lambda}{(z\bar{z})^g}, \frac{z}{\sqrt{z\bar{z}}}\right). \quad (7)$$

Through the above procedure, we get the ChP of e.g., the figure-8 knot: $f_{F8} = 1/64[64\lambda^3 - 12\lambda a^2[3(z\bar{z})^2 + 2z^2(z\bar{z}) - 2\bar{z}^2(z\bar{z})] - 14a^3(z^2 + \bar{z}^2)(z\bar{z})^2 - a^3(z^4 - \bar{z}^4)(z\bar{z})]$ with $a = 1/4$. Expanding the ChP in the series of λ takes the form: $f(\lambda, z) = \lambda^n - \sum_{j=0}^{n-1} \zeta_j(z) \lambda^j$. It is clear at the location of EP_n , $z = 0$, $\zeta_j(z) = 0$. A natural choice of the knotted Hamiltonian is

$$H_{\mathcal{K}}(z) = \begin{pmatrix} \zeta_{n-1}(z) & \dots & \zeta_1(z) & \zeta_0(z) \\ 1 & 0 & 0 & 0 \\ 0 & \ddots & \ddots & 0 \\ 0 & 0 & 1 & 0 \end{pmatrix}_{n \times n}. \quad (8)$$

Obviously $\det[\lambda - H_{\mathcal{K}}(z)] = f(\lambda, z)$. Fig. 1(d) depicts an EP_3 with its nearby energy levels forming a figure-8 knot, described by braid word $(\tau_1^{-1}\tau_2)^2$. Fig. 1(e) depicts an EP_4 associated with $L6a1$ link of braid word

$(\tau_1^{-1}\tau_3^{-1}\tau_2)^2$. By further replacing $k_{1,2}$ with $\sin k_{x,y}$ in $H_{\mathcal{K}}(z)$, we get a 2D lattice Hamiltonian hosting the desired EP_n with \mathcal{K} knot topology.

Bulk Fermi arc & discriminant number.—A direct physical consequence of the EP topology is the appearance of bulk Fermi arcs [55]. For example, a pair of EPs split from a Dirac point is connected by an open-ended Fermi arc, as identified as the isofrequency contour in photonic experiments [55]. Here we extend this notion to generic higher-order EPs and define the bulk Fermi arcs as the loci in the (k_1, k_2) space when any two levels have the same real energy, i.e., $\text{Re}[z_i] = \text{Re}[z_j]$ for $i \neq j$. As the EP satisfies this condition, a bulk Fermi arc must start from an EP and end at another; The EPs are the endpoints of Fermi arcs. The constraint imposed by the condition $\text{Re}[z_i] = \text{Re}[z_j]$ yields some 1D loci in the (k_1, k_2) space. The bulk Fermi arcs trace open-ended curves emanating from the EPs. From the braid representation, the bulk Fermi arc is formed whenever there is a crossing, either over or under, in the braid diagram. Hence we have:

$$n_{\text{arc}} = n_+ + n_- = c(\mathcal{K}). \quad (9)$$

Here n_{\pm} denotes the number of over/under crossings, respectively. $c(\mathcal{K})$ is the knot crossing number. The number of Fermi arcs n_{arc} emanating from each EP equals to $c(\mathcal{K})$ associated with the EP.

Moreover, the braid crossing dictates the discriminant invariant ν [40]. In its neat form, ν is the sum of band vorticity [39] for any pair of band:

$$\nu = -\frac{1}{2\pi} \sum_{i \neq j} \oint_{\Gamma} \nabla_{\mathbf{k}} \arg(z_i - z_j) \cdot d\mathbf{k}. \quad (10)$$

Along the closed path Γ , the EP knot contributes to the vorticity through braid crossings. An over/under crossing contributes a ± 1 , yielding

$$\nu = n_+ - n_- = W(\mathcal{K}), \quad (11)$$

where $W(\mathcal{K}) \equiv n_+ - n_-$ is the writhe of the knot \mathcal{K} . It is obvious two different EPs of different braids may have the same discriminant number, e.g., figure-8 and Borromean ring ($L6a4$). We stress that, the full information of an EP is encoded in its knot structure; either the bulk Fermi arc or discriminant number is determined by the braiding and has limited discriminant power to specify an EP.

No-go theorem.—The knot classification assigns a specific braiding pattern to a given EP. On a 2D lattice, there may exist multiple different EPs featuring distinct braidings. So what kind of EP configurations is allowed? It turns out the possible EPs on a 2D lattice are governed by the following *no-go theorem*:

$$b_1 b_2 \dots b_J \in [B_n, B_n], \quad (12)$$

where J is the total number of isolated EPs in the 2D BZ [see Fig. 2(a)], b_j is the braid for the j -th EP along a small surrounding path. $[B_n, B_n] = \{uvu^{-1}v^{-1} | (u, v) \in$

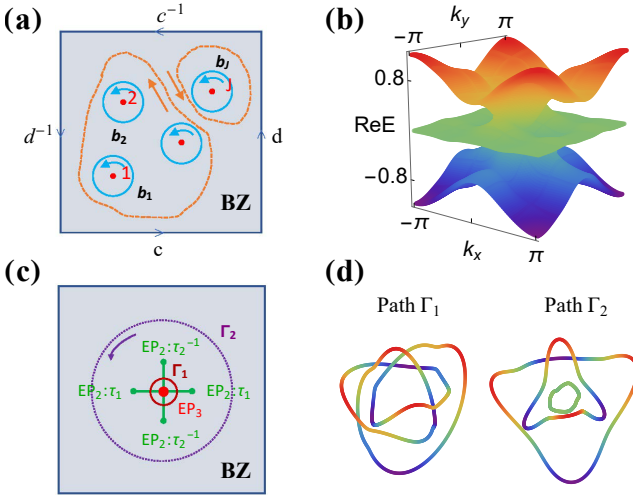


FIG. 2. Non-Hermitian no-go theorem on a 2D lattice. (a) Sketch of the proof of the theorem. The j -th EP ($j = 1, 2, \dots, J$) is labeled by level braiding b_j along the nearby path (cyan). The paths can be continuously deformed to the orange curves and finally to the BZ boundary. (b) Band structure of model (13). $m = 0.3$. (c) EPs and their associated Fermi arcs. The EP₃ of figure-8 knot (red dot) at the origin connects with the four neighboring 2-fold EPs (green dots) through bulk Fermi arcs (green lines). (d) Knots formed along the red path Γ_1 (left panel) and purple path Γ_2 (right panel) in (c).

B_n } is the commutator subgroup. It is easy to check taking a conjugate element of any b_i or switching its order in Eq. (12) is irrelevant [56]. We can continuously expand and deform the enclosing path to the Brillouin zone (BZ) boundary as sketched in Fig. 2(a), without passing through any singularity. The resulting overall band braiding $b_1 b_2 \dots b_J$ equals to the band braiding $cdc^{-1}d^{-1}$ along the four edges of the BZ as the upper (left) and lower (right) edge are identical. Specifically, if the two neighboring braidings c, d (or two braidings along any orthogonal line cut of the BZ) commute, the composite braiding must be trivial $b_1 b_2 \dots b_J = I$.

The no-go theorem indicates that the braiding of the EP inside the BZ is determined by that of the boundary. It dictates the possible braiding configurations of the isolated EPs and imposes strong constraints on their splittings: the no-go theorem holds for all the isolated split EPs, e.g., a Dirac point splits into two EPs of opposite charges. Note that the commutator subgroup is the set of braids with total exponent sum zero in the braid generator τ_i . According to Eq. (11), the doubling theorem [40] naturally arises: the sum of the discriminant number of all EPs vanishes. Hence a single EP of non-zero discriminant invariant must be paired with another one of opposite discriminant number.

We illustrate the no-go theorem through an explicit model:

$$H = H_{F8} + m \begin{pmatrix} c_{x,y} & 0 \\ 1 - c_{x,y} & -c_{x,y} \end{pmatrix} \oplus 0_{1 \times 1}, \quad (13)$$

with $c_{x,y} = 2 - \cos k_x - \cos k_y$. Here H_{F8} is the lattice Hamiltonian of the figure-8 EP given in Eq. (8). Without the second term, H_{F8} hosts four EP₃ located at $(0, 0)$, $(0, \pi)$, $(\pi, 0)$, and (π, π) , respectively. For a finite m , only the EP₃ at $(0, 0)$ survives. A typical band structure is depicted in Figs. 2(b)(c) for $m = 0.3$. Besides the EP₃ of figure-8 knot with braid word $(\tau_1^{-1}\tau_2)^2$ at the origin, four isolated 2-fold EPs, with braid word $\tau_1, \tau_2^{-1}, \tau_1$, and τ_2^{-1} , respectively, emerge nearby. Each EP₂ connects to the central EP₃ through a bulk Fermi arc. The number of Fermi arc emanating from each EP coincides with the knot crossing number [see Eq. (9)]. The knot along a closed path is shown in Fig. 2(d). If the loop is small, enclosing only the central EP₃, the energy levels close to a figure-8 knot. In contrast, if the loop encloses all the EPs, the knot is composed of three unlinked components (i.e., trivial braiding) since $\tau_2^{-1}\tau_1(\tau_1^{-1}\tau_2)^2\tau_2^{-1}\tau_1 = I$, consistent with the no-go theorem.

Discussions.—To conclude, we have established a homotopy classification of isolated EPs and demonstrated that the knots tied up by energy levels fully characterize the 2D EPs. Based on this new classification scheme, we have demonstrated how to construct NH Hamiltonians corresponding to a given knot. We further proposed a no-go theorem for the EPs on a 2D lattice. Our scheme elegantly relates the bulk Fermi arc and discriminant number to the crossing number and writhe of the knot, respectively.

The various EP knots and their associated NH Hamiltonians could in principle be realized in platforms such as photonic lattice [26, 57, 58] or electric circuits [59–63]. For the former, the asymmetric coupling between the ring resonators can be implemented via auxiliary microring cavities. The consequent bulk Fermi arcs should be extracted through resonances in frequencies [55]. For the latter, the NH Hamiltonian is simulated by the circuit Laplacian, with its band structures given by the admittance spectra. Recently, it was shown under certain symmetries, e.g., parity-time or charge-conjugation parity symmetry, higher-order EPs are stable [64, 65]. We will leave it for future work to explore the stability of knotted EPs in the presence of different symmetries. The various knotted EPs discovered here should naturally emerge as the critical point of the nonreciprocal phase transition [37]. Beyond the isolated EPs considered here, more intricate line- or surface-degeneracies may exist. For example, in 2D, encircling the EP line yields the so-called singular knots. It would be interesting to extend the analysis to such singular knots and reveal their physical consequences.

This work is supported by the NSFC under Grants No.11974413 and the Strategic Priority Research Program of Chinese Academy of Sciences under Grant No. XDB33000000.

* hhu@iphy.ac.cn

[1] C. M. Bender, Making sense of non-Hermitian Hamiltonians, *Rep. Prog. Phys.* **70**, 947 (2007).

[2] I. Rotter, A non-Hermitian Hamilton operator and the physics of open quantum systems, *J. Phys. A: Math. Theor.* **42**, 153001 (2009).

[3] V. M. Martinez Alvarez, J. E. Barrios Vargas, M. Berdakin, and L. E. F. Foa Torres, Topological states of non-Hermitian systems, *Eur. Phys. J. Spec. Top.* **227**, 1295 (2018).

[4] R. El-Ganainy, K. G. Makris, M. Khajavikhan, Z. H. Musslimani, S. Rotter, and D. N. Christodoulides, Non-Hermitian physics and PT symmetry, *Nat. Phys.* **14**, 11 (2018).

[5] E. J. Bergholtz, J. C. Budich, and F. K. Kunst, Exceptional Topology of Non-Hermitian Systems, *Rev. Mod. Phys.* **93**, 15005 (2021).

[6] N. Moiseyev, *Non-Hermitian Quantum Mechanics* (Cambridge University Press, New York, 2011).

[7] A. Ghatak and T. Das, New topological invariants in non-Hermitian systems, *J. Phys.: Condens. Matter* **31**, 263001 (2019).

[8] L. E. F. Foa Torres, Perspective on Topological States of Non-Hermitian Systems, *J. Phys. Mater.* **3**, 014002 (2019).

[9] Y. Ashida, Z. Gong, and Masahito Ueda, Non-Hermitian Physics, *Advances in Physics* **69**, 3 (2020).

[10] K. G. Makris, R. El-Ganainy, D. N. Christodoulides, and Z. H. Musslimani, Beam Dynamics in \mathcal{PT} Symmetric Optical Lattices, *Phys. Rev. Lett.* **100**, 103904 (2008).

[11] A. Regensburger, C. Bersch, M.-A. Miri, G. Onishchukov, D. N. Christodoulides, and U. Peschel, Parity-time synthetic photonic lattices, *Nature (London)* **488**, 167 (2012).

[12] B. Peng, S. K. Özdemir, S. Rotter, H. Yilmaz, M. Liertzer, F. Monifi, C. M. Bender, F. Nori, and L. Yang, Loss-induced suppression and revival of lasing, *Science* **346**, 328 (2014).

[13] H. Jing, S. K. Özdemir, X.-Y. Lü, J. Zhang, L. Yang, and F. Nori, \mathcal{PT} -Symmetric Phonon Laser, *Phys. Rev. Lett.* **113**, 053604 (2014).

[14] S. Malzard, C. Poli, and H. Schomerus, Topologically Protected Defect States in Open Photonic Systems with Non-Hermitian Charge-Conjugation and Parity-Time Symmetry, *Phys. Rev. Lett.* **115**, 200402 (2015).

[15] J. M. Zeuner, M. C. Rechtsman, Y. Plotnik, Y. Lumer, S. Nolte, M. S. Rudner, M. Segev, and A. Szameit, Observation of a Topological Transition in the Bulk of a non-Hermitian System, *Phys. Rev. Lett.* **115**, 040402 (2015).

[16] Lei Xiao, Kunkun Wang, Xiang Zhan, Zhihao Bian, Kohei Kawabata, Masahito Ueda, Wei Yi, and Peng Xue, Observation of Critical Phenomena in Parity-Time-Symmetric Quantum Dynamics, *Phys. Rev. Lett.* **123**, 230401 (2019).

[17] Lei Xiao, Tianshu Deng, Kunkun Wang, Zhong Wang, Wei Yi, and Peng Xue, Observation of Non-Bloch Parity-Time Symmetry and Exceptional Points, *Phys. Rev. Lett.* **126**, 230402 (2021).

[18] B. Zhen, C. W. Hsu, Y. Igarashi, L. Lu, I. Kaminer, A. Pick, S.-L. Chua, J. D. Joannopoulos, and M. Soljačić, Spawning rings of exceptional points out of Dirac cones, *Nature (London)* **525**, 354 (2015).

[19] C. Poli, M. Bellec, U. Kuhl, F. Mortessagne, and H. Schomerus, Selective enhancement of topologically induced interface states in a dielectric resonator chain, *Nat. Commun.* **6**, 6710 (2015).

[20] S. Weimann, M. Kremer, Y. Plotnik, Y. Lumer, S. Nolte, K. G. Makris, M. Segev, M. C. Rechtsman, and A. Szameit, Topologically protected bound states in photonic parity-time-symmetric crystals, *Nat. Mater.* **16**, 433 (2017).

[21] P. St-Jean, V. Goblot, E. Galopin, A. Lemaître, T. Ozawa, L. Le Gratiet, I. Sagnes, J. Bloch, and A. Amo, Lasing in topological edge states of a one-dimensional lattice, *Nat. Photon.* **11**, 651 (2017).

[22] L. Xiao et al., Observation of topological edge states in parity-time-symmetric quantum walks, *Nat. Phys.* **13**, 1117 (2017).

[23] X. Zhan, L. Xiao, Z. Bian, K. Wang, X. Qiu, B. C. Sanders, W. Yi, and P. Xue, Detecting Topological Invariants in Nonunitary Discrete-Time Quantum Walks, *Phys. Rev. Lett.* **119**, 130501 (2017).

[24] C. E. Ruter, K. G. Makris, R. El-Ganainy, D. N. Christodoulides, M. Segev, and D. Kip, Observation of parity-time symmetry in optics, *Nat. Phys.* **6**, 192 (2010).

[25] R. El-Ganainy, K. G. Makris, M. Khajavikhan, Z. H. Musslimani, S. Rotter, and D. N. Christodoulides, Non-Hermitian physics and PT symmetry, *Nat. Phys.* **14**, 11 (2018).

[26] H. Hu, E. Zhao, and W. V. Liu, Dynamical signatures of point-gap Weyl semimetal, [arXiv:2107.02135](https://arxiv.org/abs/2107.02135).

[27] J. Bartlett, H. Hu, and E. Zhao, Illuminating the bulk-boundary correspondence of a non-Hermitian stub lattice with Majorana stars, *Physical Review B* **104**, 195131 (2021).

[28] M. Michael Denner, Anastasiia Skurativska, Frank Schindler, Mark H. Fischer, Ronny Thomale, Tomáš Bzdušek, and Titus Neupert, Exceptional Topological Insulators, *Nat. Commun.* **12**, 5681 (2021).

[29] W. D. Heiss, The physics of exceptional points, *J. Phys. Math. Gen.* **45**, 444016 (2012).

[30] M.-A. Miri and A. Alù, Exceptional points in optics and photonics, *Science* **363**, eaar7709 (2019).

[31] Z. Lin, H. Ramezani, T. Eichelkraut, T. Kottos, H. Cao, and D. N. Christodoulides, Unidirectional Invisibility Induced by PT-Symmetric Periodic Structures, *Phys. Rev. Lett.* **106**, 213901 (2011).

[32] J. Wiersig, Sensors operating at exceptional points: General theory, *Phys. Rev. A* **93**, 033809 (2016).

[33] W. Chen, S. K. Özdemir, G. Zhao, J. Wiersig, and L. Yang, Exceptional points enhance sensing in an optical microcavity, *Nature (London)* **548**, 192 (2017).

[34] M. P. Hokmabadi, A. Schumer, D. N. Christodoulides, and M. Khajavikhan, Non-Hermitian ring laser gyroscopes with enhanced Sagnac sensitivity, *Nature (London)* **576**, 70 (2019).

[35] H. Hodaei, M.-A. Miri, M. Heinrich, D. N. Christodoulides, and M. Khajavikhan, Parity-time-symmetric microring lasers, *Science* **346**, 975–978 (2014).

[36] L. Feng, Z. J. Wong, R.-M. Ma, Y. Wang, and X. Zhang, Single-mode laser by parity-time symmetry breaking, *Science* **346**, 972–975 (2014).

[37] Michel Fruchart, Ryo Hanai, Peter B. Littlewood, and Vincenzo Vitelli, Non-reciprocal phase transitions, *Nature* **592**, 363–369 (2021).

[38] K. Kawabata, T. Bessho, and M. Sato, Classification of Exceptional Points and Non-Hermitian Topological Semimetals, *Phys. Rev. Lett.* **123**, 066405 (2019).

[39] Huitao Shen, Bo Zhen, and Liang Fu, Topological Band Theory for Non-Hermitian Hamiltonians, *Phys. Rev. Lett.* **120**, 146402 (2018).

[40] Z. Yang, A.P. Schnyder, J. Hu, and C. K. Chiu, Fermion Doubling Theorems in Two-Dimensional Non-Hermitian Systems for Fermi Points and Exceptional Points, *Phys. Rev. Lett.* **126**, 086401 (2021).

[41] C. C. Wojcik, X.-Q. Sun, T. Bzdušek, and S. Fan, Homotopy characterization of non-Hermitian Hamiltonians, *Phys. Rev. B* **101**, 205417 (2020).

[42] Z. Li and R. S. K. Mong, Homotopical classification of non-Hermitian band structures, *Phys. Rev. B* **103**, 155129 (2021).

[43] H. Hu and E. Zhao, Knots and Non-Hermitian Bloch Bands, *Phys. Rev. Lett.* **126**, 010401 (2021).

[44] Kai Wang, Avik Dutt, Charles C. Wojcik, and Shanhui Fan, Topological complex-energy braiding of non-Hermitian bands, *Nature* **598**, 59–64 (2021).

[45] Shunyu Yao and Zhong Wang, Edge States and Topological Invariants of Non-Hermitian Systems, *Phys. Rev. Lett.* **121**, 086803 (2018).

[46] J. S. Birman and J. Cannon, *Braids, Links, and Mapping Class, Groups* (Princeton University Press, Princeton, 1974).

[47] L. H. Kauffman, *Knots and Physics*, 3rd ed. (World Scientific, Singapore, 2001).

[48] E. Fadell and L. Neuwirth, Configuration spaces, *Math. Scand.* **10**, 111 (1962).

[49] A. Hatcher, *Algebraic Topology* (Cambridge University Press, Cambridge, 2002).

[50] C. Kassel and V. Turaev, *Braid Groups* (Springer, Berlin, 2008), see Theorem 2.1 on page 54.

[51] V. F. R. Jones, A polynomial invariant for knots via von Neumann algebras, *Bull. Am. Math. Soc.* **12**, 103 (1985).

[52] S. Akbulut and H. King, All knots are algebraic, *Commentarii Mathematici Helvetici* **56**, 339 (1981).

[53] B. Bode and M. R. Dennis, Constructing a polynomial whose nodal set is any prescribed knot or link, *Journal of Knot Theory and Its Ramifications* **28**, 1850082 (2019).

[54] B. Bode, M. R. Dennis, D. Foster and R. P. King, Knotted fields and explicit fibrations for lemniscate knots, *Proc. R. Soc. A.* **473**, 20160829.

[55] H. Zhou, C. Peng, Y. Yoon, C. W. Hsu, K. A. Nelson, L. Fu, J. D. Joannopoulos, M. Soljačić, and B. Zhen, Observation of bulk Fermi arc and polarization half charge from paired exceptional points, *Science* **359**, 1009 (2018).

[56] This is due to the fact that for any $x, y \in B_n$, (1) $x[u, v]x^{-1} = [xux^{-1}, xvx^{-1}] \in [B_n, B_n]$; (2) $yb_1y^{-1}b_2...b_J = (yb_1y^{-1}b_1^{-1})(b_1b_2...b_J) = [y, b_1][u, v] \in [B_n, B_n]$; and (3) $b_{i+1}b_i = b_i^{-1}(b_i b_{i+1})b_i$.

[57] S. Longhi, D. Gatti, and G. D. Valle, Robust light transport in non-Hermitian photonic lattices, *Sci. Rep.* **5**, 13376 (2015).

[58] S. Mittal, V. V. Orre, G. Zhu, M. A. Gorlach, A. Poddubny, and M. Hafezi, Photonic quadrupole topological phases, *Nature Photonics* **13**, 692–696 (2019).

[59] S. Imhof et al., Topoelectrical-circuit realization of topological corner modes, *Nat. Phys.* **14**, 925 (2018).

[60] T. Helbig, T. Hofmann, C. H. Lee, R. Thomale, S. Imhof, L. W. Molenkamp, and T. Kiessling, Band structure engineering and reconstruction in electric circuit networks, *Phys. Rev. B* **99**, 161114(R) (2019).

[61] E. Zhao, Topological circuits of inductors and capacitors, *Annals of Physics*, **399**, 289 (2018).

[62] C. H. Lee, S. Imhof, C. Berger, F. Bayer, J. Brehm, L. W. Molenkamp, T. Kiessling, and R. Thomale, Topoelectrical Circuits, *Commun. Phys.* **1**, 39 (2018).

[63] C. H. Lee et al., Imaging nodal knots in momentum space through topoelectrical circuits, *Nat. Commun.* **11**, 4385 (2020).

[64] P. Delplace, T. Yoshida, and Y. Hatsugai, Symmetry-Protected Multifold Exceptional Points and their Topological Characterization, *Phys. Rev. Lett.* **127**, 186602 (2021).

[65] Ipsita Mandal and Emil J. Bergholtz, Symmetry and Higher-Order Exceptional Points, *Phys. Rev. Lett.* **127**, 186601 (2021).